Modelling of a real CO_2 booster installation and evaluation of control strategies for heat recovery applications in supermarkets

Emilio José Sarabia Escriva[a], Salvador Acha [b], Niccolo LeBrun[b], Víctor Soto Francés[a], Jose Manuel Pinazo Ojer[a], Christos N. Markides[b], Nilay Shah[b]

[a]*Termodinàmica Aplicada, Universitat Politècnica de València, 46022 València, Spain*

[b]*Department of Chemical Engineering, Imperial College London, London SW7 2AZ, UK*

Corresponding author. *Email address:* emsaes@upvnet.upv.es (Emilio José Sarabia Escriva)

Abstract

This paper compares and quantifies the energy, environmental and economic benefits of various control strategies recovering heat from a CO_2 booster system in a supermarket for space heating with the purpose of understanding its potential for displacing natural gas fuelled boilers. A theoretical steady-state model that simulates the behaviour of the CO_2 system is developed and validated against field measurements obtained from an existing refrigeration system in a food-retail building located in the United Kingdom. Five heat recovery strategies are analysed by modifying the mass flows and pressure levels in the condenser. The model shows that a reduction of 48% in natural-gas consumption is feasible by the installation of a de-superheater and without any advanced operating strategy. However, the CO_2 system can fully supply the entire space-heating requirement by adopting alternative control strategies, albeit by penalising the coefficient of performance (COP) of the compressor. Results show that the best energy strategy can reduce total consumption by 32%, while the best economic strategy can reduce costs by 6%. Findings from this work suggest that heat recovery systems can bring substantial benefits to improve the overall efficiency of energy-intensive buildings; although trade-offs need to be carefully considered and further analysed before embarking on such initiatives.

Keywords: food retail, energy saving, transcritical R744 refrigeration, commercial refrigeration, heat recovery

Nomenclature	
A, B, C, D	Performance coefficients
AHU	Air handling unit
BPIE	Buildings Performance Institute Europe
COP	Coefficient of performance [-]
DEVS	Discrete event simulation
GHG	Greenhouse gas
GWP	Global warming potential
h	Enthalpy per unit of mass [$kJ \cdot kg^{-1}$]
DS	De-superheater

HFC	Hydrofluorocarbon
HP	High pressure
LP	Low pressure
LT	Low temperature
LTHW	Low-temperature hot water
MT	Medium temperature
$\dot{m}$	Mass flow rate [kg·s^{-1}]
ODP	Ozone depletion potential
P	Pressure [bar]
$\dot{Q}$	Heat transfer rate [kW]
T	Temperature [^{o}C]
$\dot{W}$	Power [kW]
Greek symbols	
η	Efficiency [-]
τ	Compression ratio [-]
Subscripts and superscripts	
comp	Compressor
evap	Evaporator
ext	External
gc	Gas cooler/condenser
HP	High pressure
HR	Heat recovery
is	Isentropic
LP	Low pressure
LT	Low temperature
LTHW	Low temperature hot water
MT	Medium temperature
me	Mechanical
vol	Volumetric

1. Introduction

The refrigeration and air conditioning sector was responsible for 11.6 $MtCO_2$ equivalent gas emissions in the UK during 2017 [1]. This value is similar to that of 2009 and it represents a second consecutive year of reduction in this sector. The Buildings Performance Institute Europe (BPIE) published in 2011 a report that indicated that 28% of the final energy used in non-residential building corresponded to wholesale and commercial retail trade operations [2]. Besides a significant indirect contribution to global warming, supermarket applications also have a considerable direct environmental impact due to the use of high Global Warming Potential (GWP) refrigerants, i.e. hydrofluorocarbons (HFCs). The attempt by some governments to mitigate greenhouse gas (GHG) emissions in the atmosphere is making natural refrigerants regain importance in refrigeration facilities [3]. The European regulation, known as F-gas, aims to gradually reduce the use of HFCs by about two thirds by 2030 compared to 2010 emissions [4]. This regulation requires, since January 2022, the use of refrigerants with a GWP limit of 150 for multipack centralized refrigeration systems for commercial use with a rated capacity ≥ 40 kW. This means that some gases like the R-404A, with a GWP of 3922, can no longer be used for new equipment.

In food retail operations, refrigeration system units employing CO_2 (R744) refrigerant can provide a solution to the use of high carbon footprint from conventional HFCs refrigerants [5], such as R-507A and R-404A. Apart from being environmentally friendly (GWP=1, ODP=0), inexpensive, non-toxic and non-flammable, CO2 also offers the possibility of favourably recovering heat for space and tap water heating purposes [6]. Heat recovery applications from the CO2 cycle has increased in interest: Arias and Lundqvist [7] studied in 2005 the heat recovery possibilities in Swedish supermarkets using simulated heating demands. It was one of the firsts works in this field and they obtained the best results combining floating condensing temperature and heat recovery. Cecchinato et al. [8] in 2010 proposed and evaluated different alternatives to integrate the air conditioning service with the refrigeration system and their findings estimated annual energy saving higher than 15% in colder climates. Sawalha [9] in 2013 analysed the possibilities of heat recovery in Swedish supermarkets using a simple CO2 booster refrigeration system versus the most common design consisting of a R404 refrigeration system with a separate conventional R407C heat pump. The first option presented 6% lower annual energy use than the conventional combination with a strong influence of sub-cooling after the gas cooler on the overall energy performance. Colombo et al. [10] in 2014 modelled a booster system and calculated a demand reduction of 13% in electricity and 70% in natural gas in a UK supermarket using a system configuration with two heat exchangers before the gas cooler (one for high and the other for low temperature). Polzot et al. [11] evaluated the energy saving of using heat recovery in three different climates in Northern Italy and compared the results with a R134a/CO2 cascade refrigeration system relying on a R410A separate heat pump for space heating and hot water production. The system proposed was an efficient solution during winter, but its consumption was higher than the base case in summer. This solution shows slightly annual energy savings in colder climates, while its consumption in the warmer climate period was higher than the base case. Ge and Tassou [12] studied different control strategies for heat recovery in UK supermarkets using an all CO_2 cascade refrigeration system. Results show that it was not possible to supply all the heating requirements without a specific strategy. In the work they analyse three strategies fixing the high pressure for subcritical mode in which the only option that supplied all the required heat was the strategy operating in transcritical mode continuously.

Nordic countries were the first to adopt basic transcritical R744 supermarket booster systems because low ambient temperatures offered the possibility to operate CO2 at subcritical running modes. At these operating conditions, in fact, typical transcritical CO2 solutions can outperform the systems relying on HFCs [13]. However, the adoption of an advanced system layout is compulsory to achieve great energy efficiencies in warmer climates as well. Purohit et al. [14] compared the behaviour of different alternatives seeking a better adaptation in warmer climates. The study suggests the use of parallel compression and dedicated mechanical sub-cooling schemes for hot climates and a CO2/R1234ze(E) indirect solution for extremely hot climates. Gullo et al. [15] in 2017 studied theoretically the efficiency of different configurations in European climates. They concluded that transcritical CO2 installation with ejectors in a parallel system configuration is the most efficient solution for European retailers. In previous studies, Gullo et al. [16] analysed enhanced architectures of CO2 systems applications for European cities in warmer climates; findings indicate energy savings comparable to a CO2/R134a cascade system. Efstratiadi et al. [17] examined the advantages of water-cooled gas cooler and estimated a reduction of 3% applying the system near Leicester (UK). Greater savings can be obtained for warmer climates. Karampour et al. [18] analysed the most promising configurations detailing that in warmer climate cascade systems show more savings. Gullo et al. [5] in 2018 details a deep review on system architectures and environmental and economic evaluations of CO2 systems. These works indicate that the technological advances in CO2 refrigeration systems have positioned them as a viable solution even in warm climates; such systems are being increasingly installed in warmer climates such as southern Europe [16]. Some reports indicate that between the period of 2013 to 2016 CO_2 installations experienced an increase of around 30% per year in the food retail sector [19]. In this regard, the EU-F-Gas Regulation [4] has significantly contributed to the technological improvements and thus to the increase in the number of installations.

With regards to modelling and simulation toolkits, some studies like Arias and Lundqvist [7] and Sawalha [9] utilised a simulated heating demand estimation obtained from the CyberMart software [20], developed for calculating the thermal loads in supermarkets. Meanwhile, Mylona et al. [21] developed a model to estimate the heating demand of stores using EnergyPlus [22], which is a popular software developed for thermal building simulation. Ge and Tassou [12] applied control strategies using the heating demand obtained from SuperSim [23,24]. In the case study presented in this work, the heating and the refrigeration demand come from real actual consumption of a supermarket located in Warwickshire, England. The data used in this paper has been obtained from the web databases Enacto Insight [25] and Verisae [26] (commercial monitoring portals). The first one shows the consumption of electricity and gas associated with each sub-system in the store. The second database shows the telemetry of the refrigeration packs and the different cabinets.

The purpose behind this study is to assess the potential of heat recovery technology in UK food retail environments. Specifically, this paper proposes to: 1) accurately quantify the techno-economic benefits that such systems can provide, 2) contrasts the different configurations and operational strategies. The work presented here aims to provide answers to such questions by simulating the existing refrigeration system functioning in a supermarket and analysing the possibilities of heat recovery using different control strategies.

After setting the context and defining the problem in this introductory section the work is divided into four parts. In Section 2, the methodology for a thermodynamic model of a real CO_2 booster installation is described. The model has been validated utilizing hourly data from a real supermarket. Section 3 offers an overview of the techno-economic results of the different simulations conducted under different configurations and control strategies for heat recovery. Section 4 discusses in detail the results of the study giving an appraisal of heat recovery systems in supermarkets. Lastly, in Section 5 key conclusions and further work suggestions in this research field are covered.

2. Methodology

2.1. Refrigeration system description

A typical CO_2 booster refrigeration system installed in a retail store is composed of two identical refrigeration systems, both of them work in similar conditions. Their loads are equally distributed in medium temperature (MT) and low temperature (LT) evaporators as they both supply approximately the same number of cabinets; thus making both systems have a similar consumption. Each pack relies on R744 under the CO_2 booster system configuration depicted in Figure 1 (left), while the pressure-enthalpy diagrams of the booster are illustrated in Figure 1 (right).

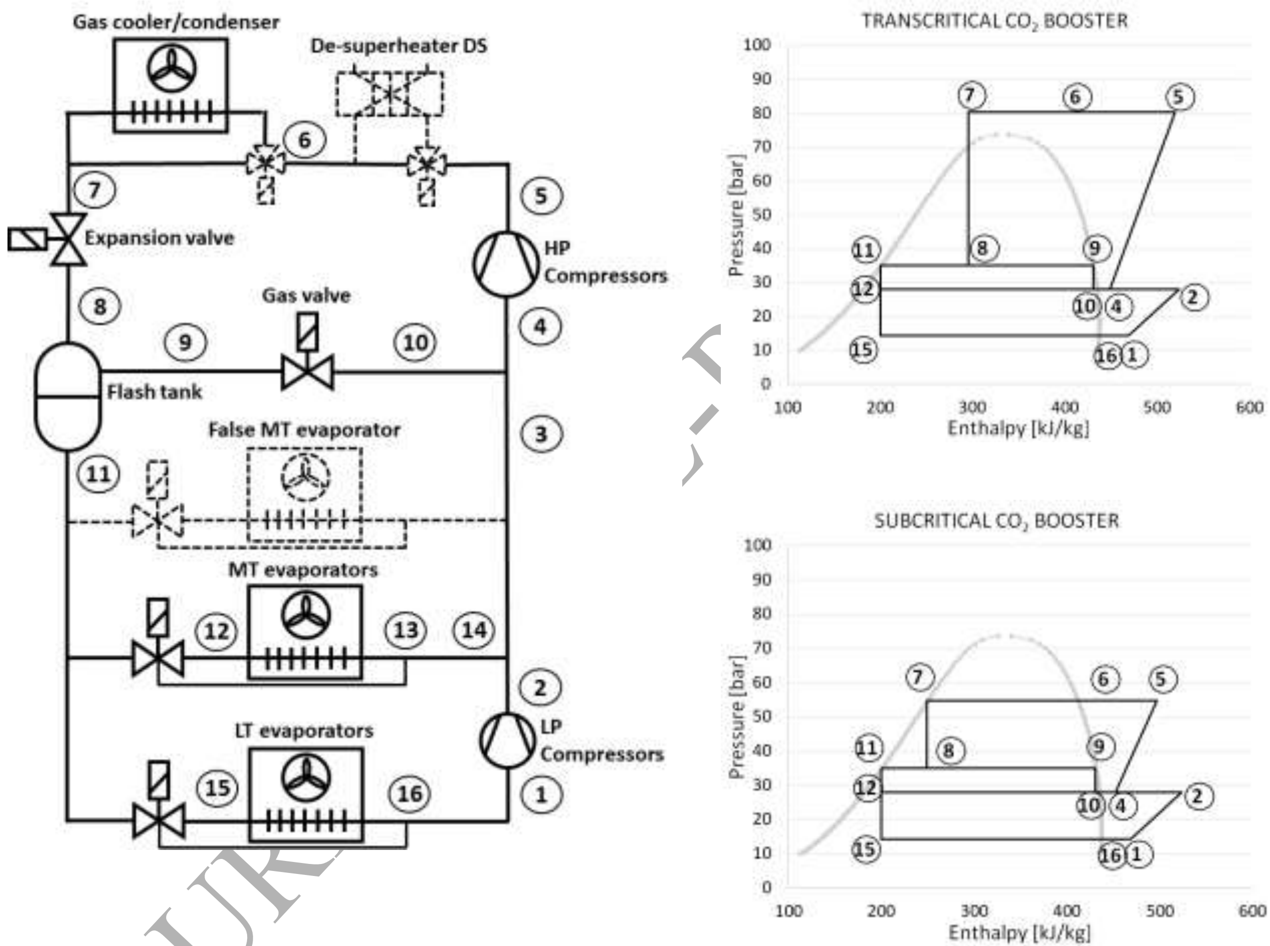

Figure 1: CO_2 booster refrigeration system (left) and its representation in the pressure-enthalpy diagram (right).

The CO_2 booster system is well known and it has been described and analysed abundantly in the literature, for example Ge and Tassou [27] analyse thermodynamically the booster cycle and evaluate the optimal high side pressure depending on the system variables. Karampour and Sawalha explained extensively this kind of system in [28]. The booster refrigeration system is a double stage compression system. The low-pressure (LP) compressors draw the super-heated vapour from the low temperature evaporators and discharge it to the pipe connected to the suction section of the high stage compressors. This suction line receives the output from the MT evaporators and the flash tank. The system works with four pressure levels which are, from lowest to highest: the LT evaporators, the MT evaporators, the flash tank and the condenser or gas cooler pressure. To recover heat from the system, additional equipment needs to be installed in a standard booster CO_2 system. The elements drawn in dashed stripes in Figure 1 (left) indicate the elements that are added to the installation allowing for recovery of the heat rejected in the condenser. The first of them is a plate heat exchanger unit (DS) situated between the high-pressure (HP) compressor outlet and the gas cooler/condenser. This DS allows to transfer heat to the supermarket heating system. In most systems, such heat exchanger unit is composed of two heat exchangers: the first heat exchanger covers the building hot water demand and the second heat exchanger is connected to the low-temperature hot water system (LTHW) and supplies space heating to the building. Within the scope of this work, we considered only space heating provision, neglecting the hot water needs of the building. This assumption is justified by the fact that building hot water is a small percentage of the overall heating demand [29]. Therefore, the heat recovered from the DS is assumed to be utilized entirely for space heating purposes. The other key element to consider for heat recovery is the false evaporator. This component has the purpose of increasing the evaporator loads and so, increasing the refrigerant mass flow throw the high-pressure part of the system in order to generate more heat in the DS. This component is necessary in case of low refrigeration demand and high heating demand. The false MT evaporator works under the same conditions as the conventional MT evaporator, for this reason its inlet and outlet points in have not been depicted Figure 1 (right).

The thermodynamic cycle is described for each element with the following equations:

- Power input in compressors

$$\dot{W}_{LP} = \frac{\dot{m}_{LP,comp}(h_2 - h_1)}{\eta_{me}} \tag{1}$$

$$\dot{W}_{HP} = \frac{\dot{m}_{HP,comp}(h_5 - h_4)}{\eta_{me}} \tag{2}$$

- Capacity of evaporators

$$\dot{Q}_{LT,evap} = \dot{m}_{LP,comp}(h_{16} - h_{15}) \tag{3}$$

$$\dot{Q}_{MT,evap} = \dot{m}_{MT,evap}(h_{13} - h_{12}) \tag{4}$$

- Heat recovery rate

$$\dot{Q}_{HR} = \dot{m}_{HP,comp}(h_5 - h_6) \tag{5}$$

- Heat rejection rate in gas cooler/condenser

$$\dot{Q}_{GC} = \dot{m}_{HP,comp}(h_6 - h_7) \tag{6}$$

- Mass balance in the cycle

$$\dot{m}_{HP,comp} = \dot{m}_{LP,comp} + \dot{m}_{MT,evap} + \dot{m}_9 \tag{7}$$

- The flow mass which leaves the flash tank through the gas valve is calculated doing an energy balance in the flash tank

$$\dot{m}_9 = \dot{m}_{HP,comp} \frac{h_8 - h_{11}}{h_9 - h_{11}} \tag{8}$$

2.2. *Model description*

The model described in Section 2.1 has been implemented in Scilab [30] and the refrigerant properties have been calculated using the CoolProp [31]. It consists in a steady-state model, parametrized for different variables whose values are obtained from the telemetry data of different databases. This model is used to calculate the consumption of the refrigeration system. Other consumptions related with cabinets or auxiliary elements, such as fans or lights, have not been considered. The values of the enthalpy terms in Eqs. 1-8 were calculated based on the temperatures and pressures measured in the system as follows.

The pressure in MT and LT evaporators can be considered constant across the year, which indicate that evaporators maintain a constant temperature. Figure 2 shows a period of six months with a sampling interval of five minutes. The graph indicates that the pressure in MT and LT evaporators can be considered constant across the year and equal to 14 bar for the LT evaporators (i.e. LT = -30 ºC) and to 28 bar for the MT evaporators (i.e. MT = -8 ºC); respectively. For most of the time the installation is working in subcritical operation, but there are some moments where the operation becomes transcritical (i.e. over 73.6 bar). This data has been obtained form the database Verisae [26]. This platform obtains the data from the different controllers in the system. The system controller unit is AK-SC 255 and cabinets are equipped with AK-CC550A controller. The temperature sensors used are PT1000 with a precision of ±0.3 ºC at 0 ºC, increasing ±0.005 ºC per degree. The precision of the controller is ±0.5 ºC for temperatures from -35 ºC to 25 ºC and ±1 ºC for higher temperatures. The pressure transducer used is AKS2050 with a usual precision of ±0.5% and maximum deviation of ±1%.

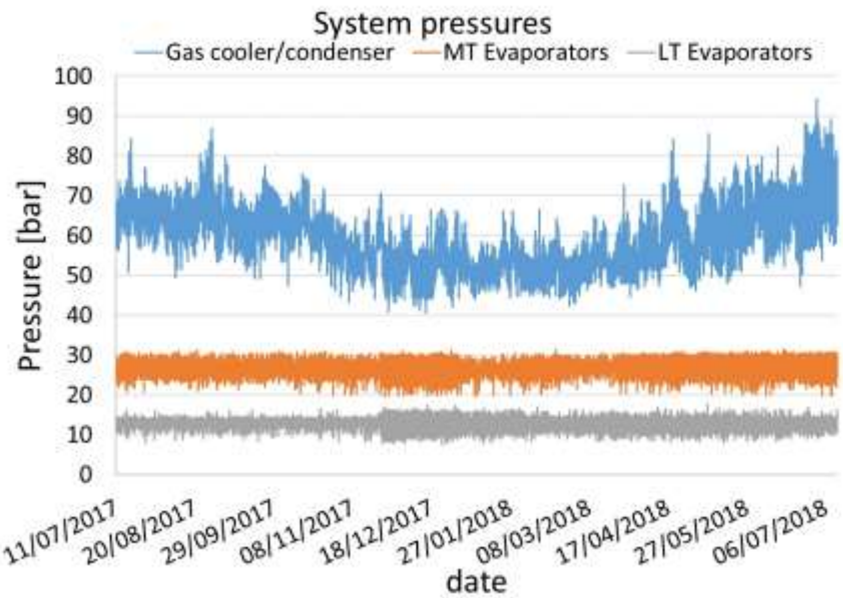

Figure 2: Pressure values in LT/MT evaporators and gas cooler/condenser from the supermarket.

The telemetry data also allows us to calculate the suction temperature of the compressors. The difference between this value and the evaporators temperature is the superheating of the evaporators. The total superheating in the LT evaporators was calculated to be 35 ºC, which is significant and is due to the large temperature difference between the refrigerant and the ambient, the long distance between evaporators and compressors, and the quality and thickness of the insulation used in the pipe. On the other hand, the MT evaporators have a superheating of 15 ºC.

The performance map of the compressor has been obtained using the data from the manufacturers. A first attempt to extract the performance from telemetry data was unsuccessful and resulted in unreasonable values for the isentropic efficiency. Upon investigation, the reason for such anomaly was identified in the signal delays from the instrumentation which made impossible to properly correlate data during transients. In addition, there were no mass flow sensors. Thus, the isentropic performance and the volumetric performance has been obtained using the results from the web application of the manufacturer (Bitzer) [32]. The installation has three LP compressors, one 2MSL-07K and two 2KSL-1K. Meanwhile, the HP group of compressors is composed of three compressors 4FTC-20K, one of them is equipped with a variable-frequency drive, in order to adjust more accurately the necessary capacity. To obtain the volumetric and isentropic performance, Eqs. (9) and (10), and the volumetric displacement of each group, four operating points for the LP compressors and eight operating points for the HP compressors have been calculated. Out of the last eight points, four of them were in subcritical operation and the other four in transcritical.

$$\eta_{vol} = 1 - A \cdot \tau \tag{9}$$

Table 1 shows the results for coefficient A in the volumetric performance equation and the total volumetric displacement for each group.

The same points used for the calculation of the volumetric performance have been used to calculate the isentropic performance. In this case, the isentropic performance has been defined by a quadratic expression, given in Eq. (10). The values obtained for each coefficient are showed in Table 1 . Using the same data to obtain the mechanical performance of the compressor, a value of 1 is used. Despite this value represents an ideal situation, this is the data provided by the manufacturer [32] and it is assumed the real data probably is near unity.

$$\eta_{is} = \frac{h_{is,outlet\ comp} - h_{inlet\ comp}}{h_{outlet\ comp} - h_{inlet\ comp}} = B + C \cdot \tau + D \cdot \tau^2 \tag{10}$$

Table 1: Volumetric displacement and coefficients for HP and LP compression groups.

	HP compressors	LP compressors
Volumetric displacement [m^3h^{-1}]	57.2530	8.2435
A	0.0912	0.1400
B	0.2985	0.4489
C	0.2719	0.1810
D	-0.0574	-0.0355

Finally, the flash tank pressure is set at 35 bar, as suggested by the contractors and we use this value to model the real behaviour of the refrigeration system. The temperature difference considered between the outlet of the gas cooler and the exterior ambient air is 8.36 ºC, this value is the average value obtained during the period showed in Figure 3.

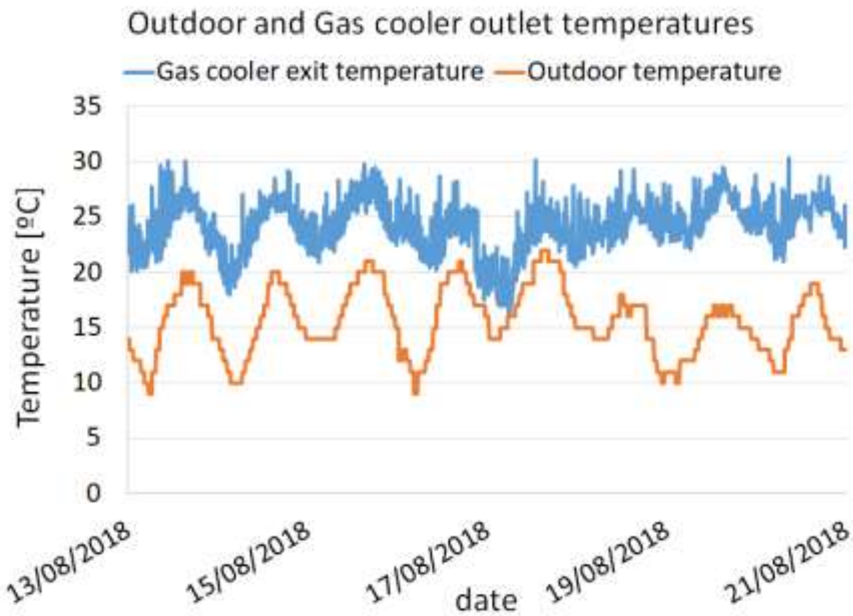

Figure 3: Outdoor and gas cooler exit temperatures from the supermarket.

The thermal loads in the shop floor cabinets depend on factors such as lighting, stocking levels, people occupancy levels, defrost cycles and store temperature among others. These thermal loads are compensated by increasing the refrigeration system cooling capacity. This refrigeration capacity depends strongly on outdoor temperatures. This interdependency studied in detail by Acha et al. [33]. For these reasons, the compressors capacity defined in the model has been calculated by taking average values depending on the outdoor temperatures and the store operating schedule (Figure 4). Equation (*11*) shows the capacity of the HP compressors. The capacity of the LP compressor is considered constant at 50% for open hours and 45% for close hours. These constant values for LP compressors' capacity are due because LT evaporators are equipped with doors and their cooling demand is therefore more stable. The store opening times are from 8:00 to 21:00 hours Monday to Saturday and 10:00 to 16:00 hours on Sunday.

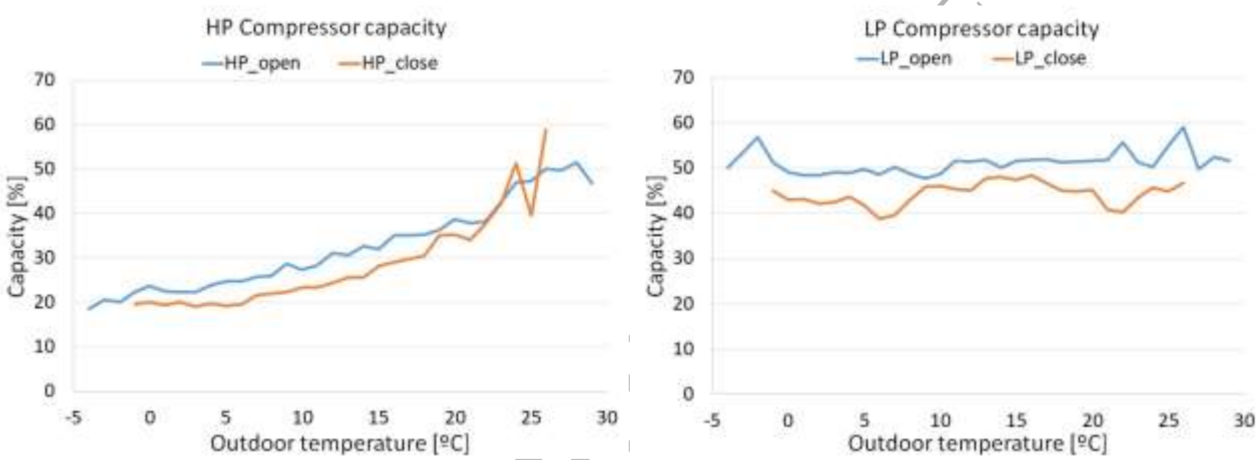

Figure 4: Average compressors' capacity related with outdoor temperature.

$$\text{HP capacity } (\%) \begin{cases} \text{open hours} \\ 0.0199 \cdot \text{Text}^2 + 0.4569 \cdot \text{Text} + 21.682 \\ \text{close hours} \\ 0.0538 \cdot \text{Text}^2 - 0.2025 \cdot \text{Text} + 18.946 \end{cases} \quad (11)$$

This data has been estimated using data values of compressor's capacity obtained from the energy-metering database Enacto [25]. The different consumption when the store is opened or closed can be observed in Figure 5, where the consumption oscillates accordingly to the time of day.

2.3. *Heating system description*

To solve the model described in the previous section the knowledge of the key system variables is required. The value of these variables has been chosen by analyzing telemetry data from the CO_2 booster in a real supermarket. The store was built in 2015 and has a total sales area of 1,600 m². It is located in the West Midlands region of the UK, Figure 5 shows the number of hours at different outdoor temperature in the region [34].

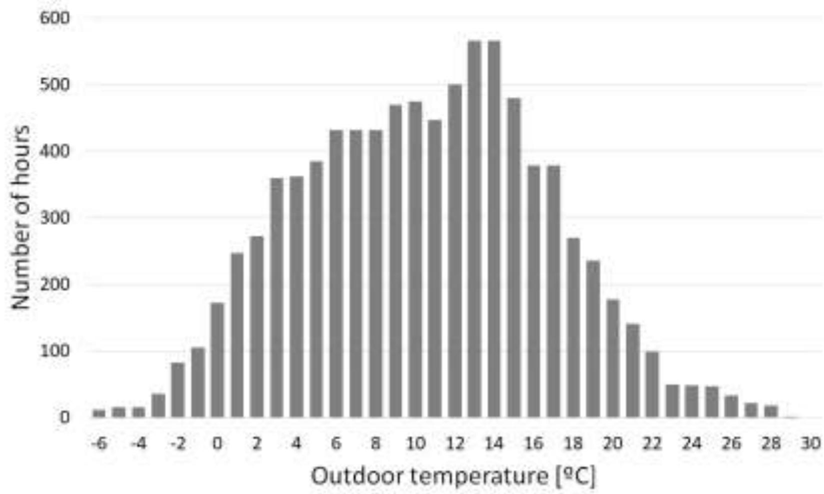

Figure 5: Hourly histogram of outdoor temperatures in West Midlands region (Warwickshire)

The actual heating system consists of a natural gas-fuelled boiler and an air handling unit (AHU) which provides the necessary warm air to the store; both systems are linked by a water circuit. The air distribution in the store is done through ducts and diffusers in a way that does not impact considerably the area of the chilled cabinets. In order to take advantage of the heat recovery, a new heating battery is added by including the heat recovery exchanger (DS) as described by Figure 6.

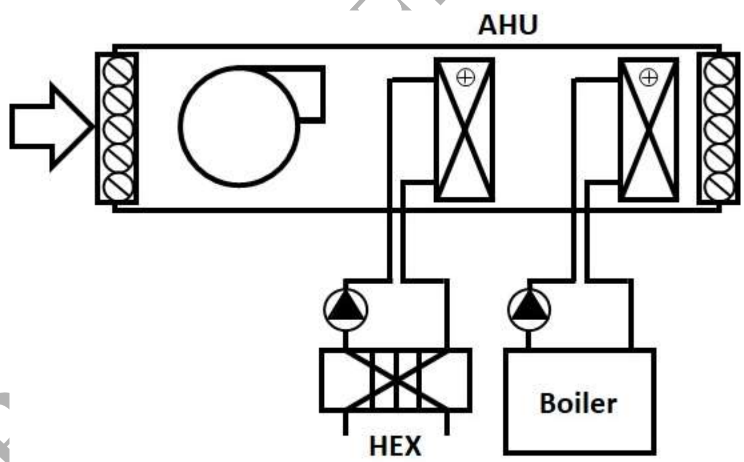

Figure 6:Heating system schematic composed by the AHU with two heating batteries, one supplied by the boiler and the other supplied by the refrigeration system.

AHU only supplies heat to the store and no cooling as space cooling requirements are rather low. In summer space cooling is provided by recirculating the cold air from the cabinets directly into the store. The heating is produced on-site by a boiler, which uses natural gas. From discussion with industrial partners it was decided to take an average boiler system efficiency of 93%; considering the boiler combustion efficiency and heat losses in distribution.

The thermostat controls in the building management system regulate the sales floor space temperature set point at 16 ºC and 19 ºC; respectively when the store is closed and opened to the public. The heating demand in the building depends on many factors, such as the weather conditions, the internal loads and the insulation of the walls and windows. For the analysed store, the annual heating demand was obtained from the energy management system database (Enacto). Figure 7 shows as an example the heating requirements against outside weather temperature for a summer and a winter week; respectively. The heating requirements starts when the store opens, at this moment, the difference between the air temperature in the store and the set-point is high; thus, in the first hour there is a peak in the heating demand. This peak is higher in winter days because the outdoor temperature is lower. During the rest of the day, the heating requirements are on average higher in winter because of the heating loads in the store depend on the outdoor temperature.

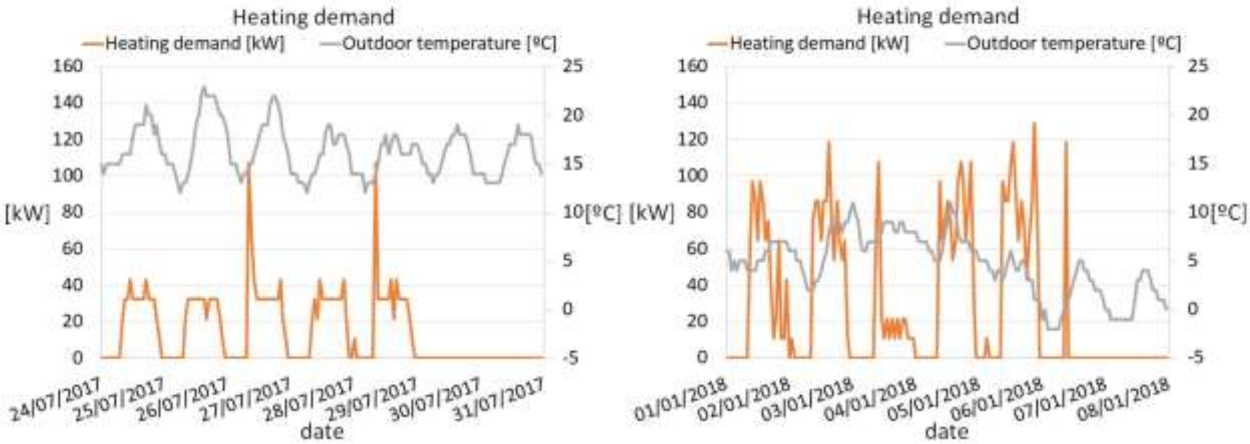

Figure 7: Heating demand for a summer week (left) and for a winter week (right).

2.4. *Simulation strategies*

The simulation conducted covers the period between 11th July 2017 to 11th July 2018. The outdoor temperature used in the simulations has been obtained from the nearest weather station from the database MIDAS [34]. The required compressor capacity has been determined by Eq. (11). The model was then applied to simulate the electrical consumption (and the space heating provided) when the CO_2 booster is used in the waste heat recovery configuration. The economic trade offs of the new system was calculated by computing the cost of electricity and heat consumption. It is necessary to point out that the economical analysis takes into account only the operational cost of running such system and not the capital costs. Therefore, the economic analysis does not consider the cost of installing the heat recovery components nor the savings from avoiding the installation of a gas boiler.

Five different heat recovery strategies have been studied, as well as a base case scenario; these are:

- Base case: relates to how the installation currently operates. The refrigeration system operates based on a floating condensing temperature while the gas is consumed by the heating system.
- Case 1: the installation operates in the same way as in the base case, but heat is recovered in the gas cooler/condenser and used to reduce the gas heating demand

when it is possible.

- Case 2: the installation tries to supply all the heating demand increasing the mass flow through the gas cooler/condenser without increasing pressure. This control only operates when heating demand is required. If there is no heating demand, the system operates as the base case.
- Case 3: the installation tries to supply all the heating demand increasing the pressure in the condenser. The pressure is increased only to the necessary level to obtain the required heat. In this case, the pressure is limited to 120 bar, if the heat recovered is not enough, the temperature in the gas cooler/condenser rises to satisfy the heating requirement. This control only operates when heating demand is required. If there is no heating demand, the system operates as the base case.
- Case 4: the installation tries to supply all the heating demand using the most efficient option described by Sawalha in [9]. The pressure is increased only to the necessary level to obtain the required heat, but this pressure has a lower limit than Case 3. In this case, the pressure limit is defined by Eq. (12). If the heating demand has not been supplied, the system increases the gas cooler outlet temperature.
- Case 5: the heating demand is supplied using the most economical option among Cases 2, 3, 4 while utilizing the boiler as a back-up when necessary. All options are considered for each time period and are evaluated to reduce costs. The cheaper option is selected each moment.

$$P_{gc} = 2.7 \cdot T_{LTHW} - 6 \tag{12}$$

In all the cases, the thermal inertia of the heating system has not been considered. The refrigeration system for Cases 2, 3 and 4 supplies the heating demand instantaneously. The temperature of the refrigerant outlet at the heat recovery exchanger (Point 6 in Figure 1) has been assumed to be 35 ºC, according to previous works [10,11].

For all cases, supply of the cooling demand is assumed to be guaranteed. In addition, the refrigerant mass flow in the LP compressors is constant in all cases and equal to the base case, and the mass flow in the HP compressors is at least the same as in the base case.

Despite the fact that the outlet temperature in the LP compressor is high, the possibility of recovering additional heat from this process was not considered. This is because the mass flow rate in the LT evaporator is low and thus the energy obtained is insignificant.

The analysis of each strategy considered energy consumption, operational costs and CO_2 equivalent emissions; thus, giving a techno-economic and environmental analysis of the impact each approach has. For the calculation of the operational cost, the prices for electricity and gas in the period analysed have been used. The gas price is constant during the year, 0.02341 $£ \cdot kW^{-1} \cdot h^{-1}$ in 2017 and 0.0256 $£ \cdot kW^{-1} \cdot h^{-1}$ in 2018. The electricity, in contrast, varies every half hour and is location dependent for each UK region. Gas and electricity prices used in this analysis are based on previous cost modelling studies [35] [36]. The coefficient used to calculate CO2 emissions is constant, 0.184 $kgCO_2 \cdot kW^{-1} \cdot h^{-1}$ for natural gas and 0.283 $kgCO_2 \cdot kW^{-1} \cdot h^{-1}$ for electricity, these values have been obtained from the UK Government [37].

3. Results and discussion

3.1. Model validation

The model has been validated by comparing the real power consumption of the installation during a year and the consumption predicted by the model. The comparison has been conducted by feeding into the model the registered outdoor temperature and the compressor capacity required. Figure 8 represents the refrigeration consumption for a summer week and a winter week. As the figure shows, the model was able to reproduce the behaviour of the refrigeration system with a good level of precision. The difference in the consumption of the installation during the hours when the store is open or closed is mainly due to the night blind curtains used during the night covering the cabinets. When the store closes, the cabinets are protected with the night blinds, thus minimizing the thermal load. During the day, these curtains are removed and the cabinets are exposed to the thermal load from lighting, people, equipment, greater air currents and higher temperatures of the store.

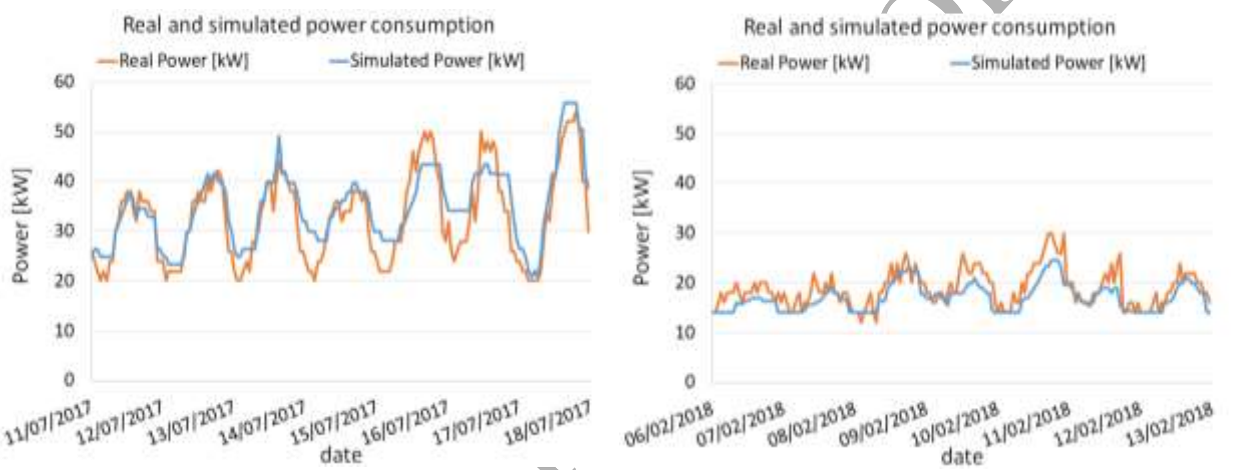

Figure 8: Real and simulated power consumption for a summer week (left) and a winter week (right) in the supermarket.

Figure 9 shows the relationship between the real and the calculated refrigeration power input versus the outdoor temperature. The simulated model shows at most two possible values of the power demand for each value of the outdoor temperature. These two values correspond to the opening hours (maximum value) and closing hours (minimum value). In contrast, the real installation shows a more complex behaviour, with a greater range of possible values due to the influence of other variables such as the variability of the evaporators thermal loads which depend on internal store operation. The model does not consider this complexity and therefore cannot capture the full variability of the refrigeration load consumption.

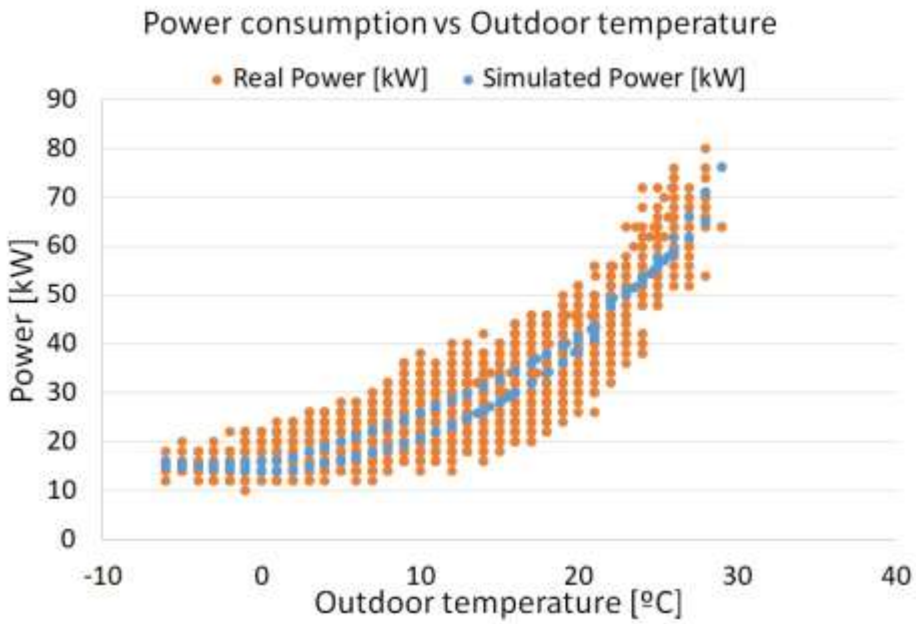

Figure 9: Pack power load vs outdoor temperature.

Nonetheless, in spite of the reduced number of variables used in the theoretical model (time and outdoor temperature), its output correlate quite well against actual demand. Table 2 shows the precision of the model. The mean average percentage error shows the deviation of the power load calculated with the theoretical model with respect to the real power load of the system. This value may seem high, but it is a positive result considering that the model uses only a limited number of variables. The annual error, in contrast, is low indicating that the annual energy consumption calculated is a good approximation.

Table 2: Model validation results.

Mean average percentage error	11%
Annual energy error	0.12%
Coefficient of determination R^2	0.86

3.2. *Evaluation of control strategies*

Key results from the various control strategies are presented in Table 3 depicting the trade-offs; detailing the economical cost of operation, the CO_2 emissions and the energy consumption.

Table 3: Annual results of costs, emissions and energy for each control strategy tested.

	Base case	**Case 1**	**Case 2**	**Case 3**	**Case 4**	**Case 5**
Natural gas cost (£)	3,746	1,952	0	0	0	1,192
Electricity cost (£)	25,381	25,381	38,410	28,416	28,338	26,093
Total cost (£)	**29,126**	**27,332**	**38,410**	**28,416**	**28,338**	**27,284**
Natural gas emissions ($kgCO_2$)	28,007	14,462	0	0	0	8,794
Electricity emissions ($kgCO_2$)	71,192	71,192	101,770	78,329	78,162	73,442

Total emissions (kgCO₂)	**99,199**	**85,654**	**101,770**	**78,329**	**78,162**	**82,237**
Natural gas demand (kWh)	152,210	78,597	0	0	0	47,795
Electricity demand (kWh)	251,563	251,563	359,611	276,780	276,190	25,9513
Energy consumption (kWh)	**403,773**	**330,160**	**359,611**	**276,780**	**276,190**	**307,309**

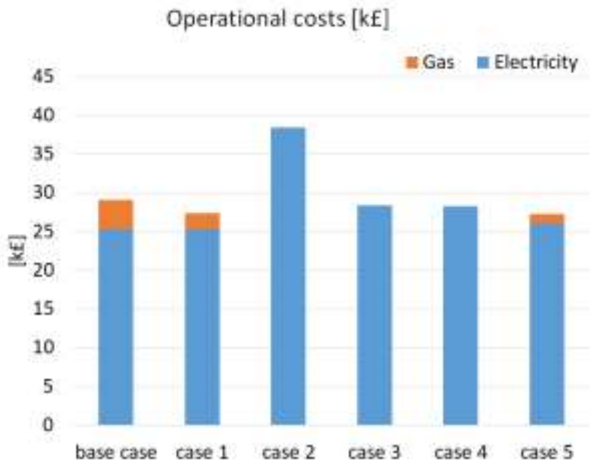

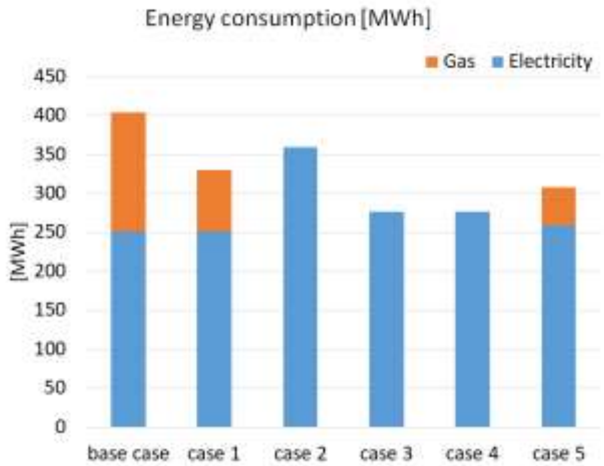

Figure 10: Operational costs in k£ (left) and energy consumption (right) for each control strategy.

Figure 10 shows the operational costs and the energy consumption for each control strategy during the simulation period. In terms of energy consumption, option 4 uses less energy than the rest. In addition, the gas installation is not necessary. But as the electricity is more expensive than gas, in terms of operational costs, Case 4 is 3.5% more expensive than Case 5. The advantage of Case 4 relative to Case 5 is that a gas installation is not necessary in the former.

It is important to consider that there are many hours during the period analyzed in which the heat rejected via the gas cooler/condenser is not employed by the heating system. In the cases analyzed, the heating demand is supplied directly, without any type of storage tank. It means that the system must supply the peaks of heating demand and it penalizes the system performance as the heat produced during the night is lost. Using thermal accumulation enables benefiting from the additional heat that is rejected from the gas cooler/condenser during hours when this heat is not needed.

3.3. *Analysis of case 1*

This case is the simplest as it uses the heat produced at the outlet of the HP compressors to supply part of the heating demand without changing the operation mode with respect to the base case. It allows for a reduction in the gas consumption, while the electrical consumption does not change. Figure 11 shows the heating demand and the potential for heat recovery for a week in summer and winter at hourly intervals. In summer, the potential for heat recovery capacity increases and it is enough to supply most of the heating demand required (Figure 11 left). Only the peaks of the first hour remain uncovered because of their high values. In contrast, the capacity of heat recovery in winter is lower while the demand increases (Figure 11 right). The refrigeration system produces annually 166.2% of the required energy from the heating system, but only 29.6% of this energy is useful for the heating system highlighting the need to improve heat recovery management strategies.

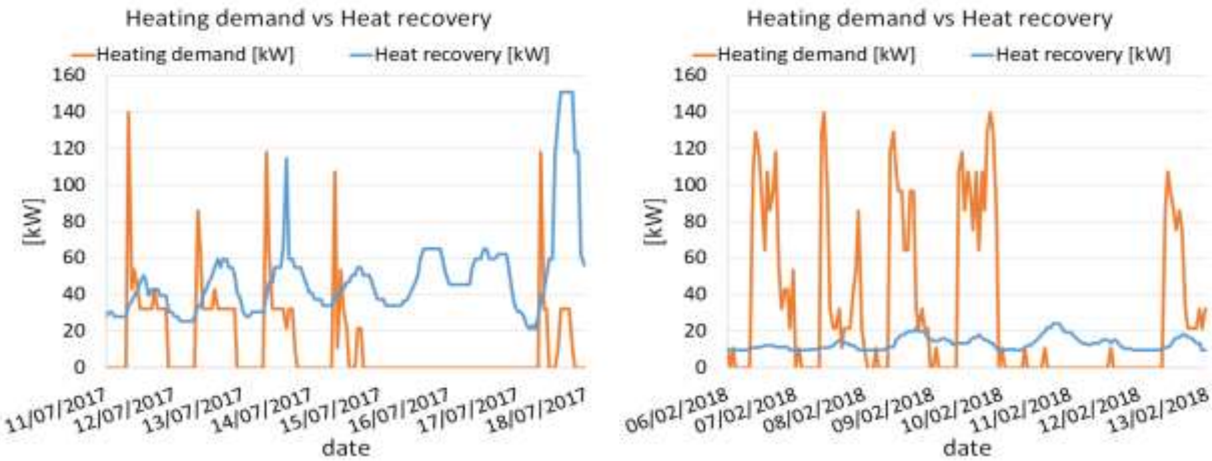

Figure 11: Heating demand and potential heat recovery in Case 1 for summer (left) and winter (right) weeks.

3.4. ***Analysis of case 2***

The second case scenario has the highest operational costs. This strategy allows transferring the necessary heat from the de-superheater to meet the heating demand and thus reduce the gas consumption; however, the strategy significantly increases the consumption of electricity. Overall, the operational costs are higher than any other control strategy considered in this work. Figure 12 shows how the system can supply all the necessary heat in summer (left) and winter (right) periods. This second case requires the installation of a false load evaporator in parallel with the MT evaporator to produce the required heat when the discharge compressor temperature is too low and the mass flow rate through the condenser (and in the false evaporator) needs to be increased. This option is less efficient than increasing the pressure because the enthalpy difference between the inlet and outlet of the de-heater is smaller when the system works in subcritical mode; thus, the useful heat in this process is low.

Figure 12 shows how this strategy works. Cases 3 and 4 have the same work mode. Both cases increase the heat in the de-superheater only when the heating demand is higher than the heat recovered in the previous case. During the hours when heating demand is zero, the potential heat profitable is lost and the system works as in the base case.

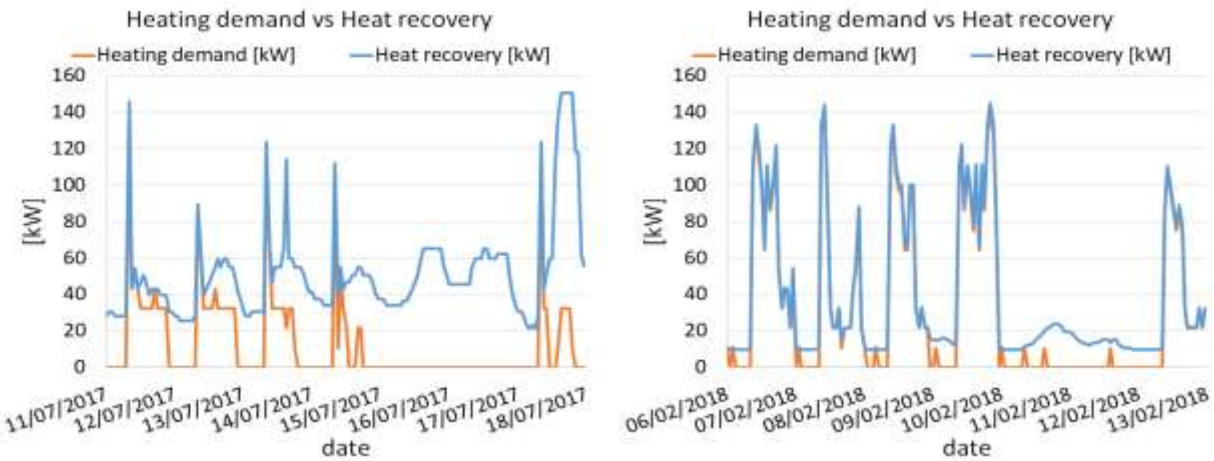

Figure 12: Heating demand and potential heat recovery in Case 2 summer (left) and winter (right) weeks.

3.5. *Analysis of case 3*

The third case control strategy can arbitrage the pressure in the HP compressors to increase the refrigerant temperature and therefore increase the supply of heat when necessary. The installation works as normal (i.e. case 1) when the heating demand is less than the heat recovered. In case the heat recovered is less than the heating demand, the system increases the HP compression ratio until the heating demand is supplied completely. This option reduces the annual energy consumption with regards to case 2 while also reducing the gas consumption to zero. Nonetheless, the increase in electricity consumption (10%) penalizes energy use and hence total costs result lower than the base case (2.4%). However, it is important to consider that in this case a boiler installation is not necessary making capital costs savings possible. This option can be beneficial in supermarkets which are planned to be built in areas where a gas connection (and a gas boiler) are absent in the first place.

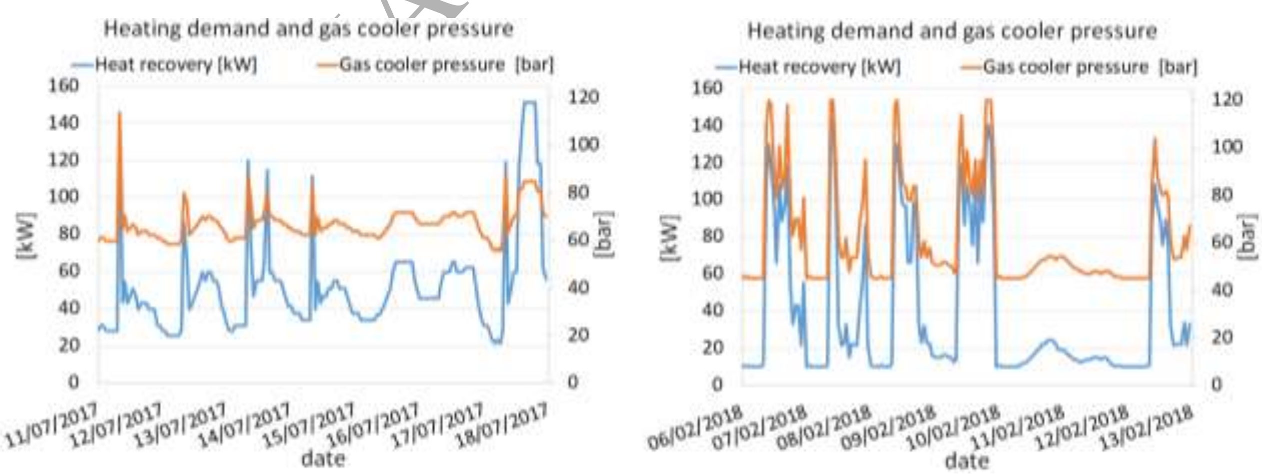

Figure 13: Heating demand and gas cooler pressure in Case 3 in summer (left) and winter (right).

The high-side pressure level required has been obtained by iterating the model until the heating demand was covered by the DS. The maximum high-side pressure was limited to 120 bar, as seen in Figure 13. This limitation means that in some instants the heat exchanged in de de-superheater is not sufficient to cover the heating demand. If that is the case, the gas cooler/condenser outlet temperature increases until the heat exchanged reaches the heating demand. It can be observed in Figure 13 (right), during the winter period, when the heating demand is high.

3.6. Analysis of case 4

The results obtained applying this control strategy are similar to the previous cases, but here, the energy consumption is slightly lower and the system works at a lower high pressure. This is because the high pressure is limited according to Eq. (12) and depends on the de-superheater outlet temperature, which is established at 35 ºC (Figure 14). This strategy was defined in [9] and it consists on following the most efficient procedure according to the system COP.

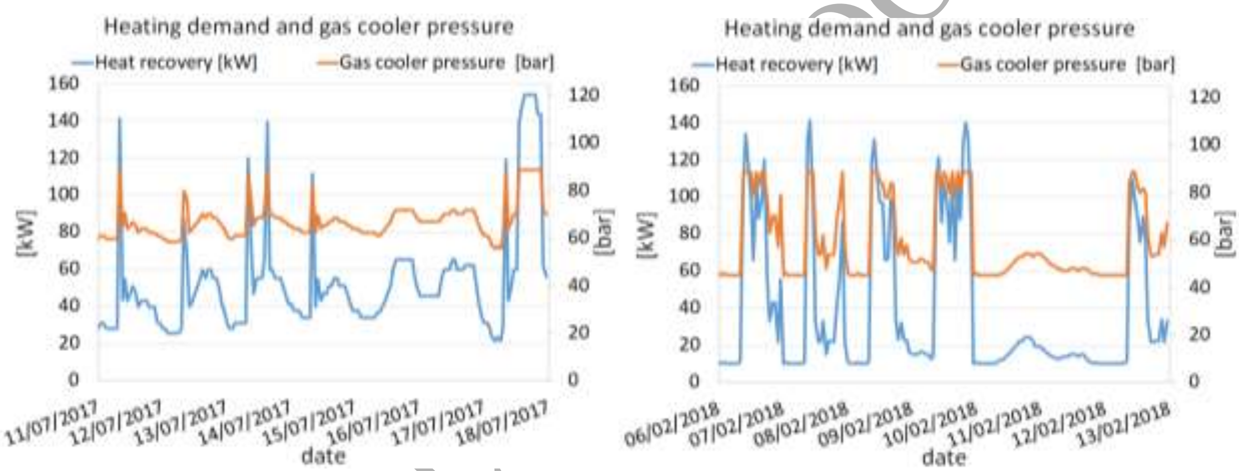

Figure 14: Heating demand and gas cooler pressure in Case 4 summer (left) and winter (right) weeks.

Case 4 shows a reduction of 2.7% in operational costs and 31.6% in energy consumption with respect to the base case. This strategy avoids the need of a gas installation. The high pressures in the system are not as higher as the case 3, as seen in Figure 14. For these reasons, this option seems to be the most suitable to implement as an alternative to the base case.

3.7. Analysis of case 5

The final case consists in choosing the most economical option among Cases 2, 3, 4 while using the gas boiler when necessary. This option has, obviously, the less operational cost, despite of the fact that the energy consumption is higher than Cases 3 and 4. In this case, the refrigeration system only tries to produce more heat in the gas cooler/condenser when it is financially worthwhile. There are some hours when it is cheaper to use the boiler than increasing the heat transferred in the de-superheater; this mainly occurs in the winter period, as shown in Figure 15 (right).

Using the case 5 strategy, the operational costs are reduced by 6.3% with respect to the base case; therefore, achieving a similar reduction to case 1. However, the solution does not avoid the use of the boiler system.

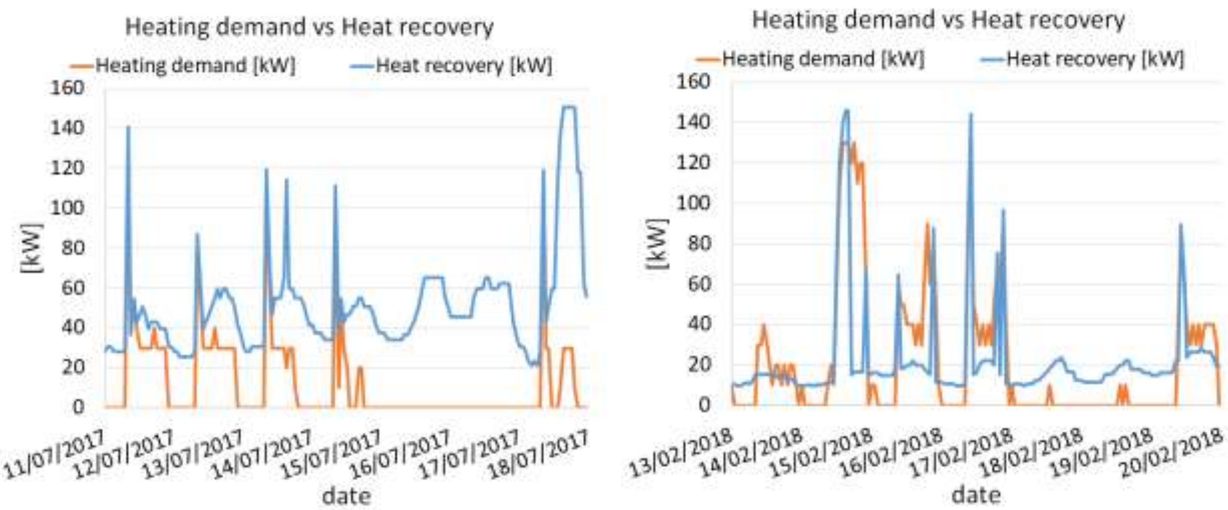

Figure 15: Heating demand and potential heat recovery in case 5 summer (left) and winter (right) weeks.

3.8. *Analysis of the installation behaviour*

The refrigeration system works constantly during all the year making possible to recover sufficient heat as needed for space heating. However, it becomes troublesome when this heat is generated in the absence of a thermal storage unit. Table 4 shows the heat recovery potential values. The first row depicts the percentage of heat sourced annually in conditions of heat recovery (more than 35 ºC) with respect to the annual heating demand, but is not sourced to match when the store requires it. The amount of heat produced in case 1 could be enough to cover the heating demand. Cases 2, 3 and 4 produce more than two times the heating demand. The second row in the Table 4 shows the portion of the heat recovered actually used to supply the heating demand. These values indicate the inefficiency of the system if no thermal storage element is placed.

Table 4: Results of costs, emissions and energy for each case.

	Case 1	**Case 2**	**Case 3**	**Case 4**	**Case 5**
% Heat recovery vs. demand	181.4%	231.7%	231.8%	235.0%	200.8%
% Useful heat recovery	28.7%	43.2%	43.1%	42.6%	35.3%

4. Conclusions

This work investigated the applicability of solutions for heat recovery from a CO2 booster system in a UK supermarket. A theoretical steady-state model has been developed, validated and tested to simulate five different control strategies for heat recovery; quantifying their performance in terms of CO_2 emissions, energy consumption and costs.

The thermodynamic model has been developed using extensive telemetry data from a real supermarket. Thus, the model is adjusted to the features of the real installation and the building analysed. Previous work has used refrigeration loads calculated with software to obtain demand estimations based on these loads. However, this paper benefits from using real data obtained from existing running equipment; hence the fidelity of the model proposed approaches real system refrigeration performance.

Five control strategies aimed at taking advantage of the heat recovery potential at the gas cooler/condenser have been analysed and compared. The first consisted of recovering the heat rejected under normal working conditions. It is a simple option that reduces natural gas demand by 48% and the operational costs by 6.2%. The most attractive option was found to be the fourth strategy (case 4). This consisted on increasing the high pressure to a defined limit in order to supply the heating demand. This fourth strategy allows savings of 32% in total energy consumption and completely avoids the use of natural gas. The most cost efficient option is the fifth strategy, which considers the use of natural gas only when the use of it is cheaper than employing the heat recovery system.

In addition to the above quantitative conclusions, the present work highlights the difficulty of following the system's behaviour with a steady-state model of the installation. Despite the annual energy consumption being accurately calculated, the hourly electric power load is not very precise due to the difficulty of having full knowledge of all operational variables in the installation. A more accurate model could be developed using other simulation methodologies such as Discrete Event Simulations (DEVS). This methodology would then allow us to obtain more accurate results by considering the system dynamics, nonetheless it requires developing a non-steady state model.

It is worth mentioning that the strategies analysed in this work did not consider the use of thermal storage, but results have shown significant heat rejected to the environment that can be utilized for other things aside from space heating. The first case, for example, produced more than 180% of the heating demand, but only 29% of this energy was used. For this reason, future studies should focus on integrating thermal storage into these systems in order to examine how this can improve savings and primary use of energy; helping support the decarbonisation of food retail buildings.

Acknowledgements

This research was supported by funds provided via the Imperial–Sainsbury's Supermarkets Ltd. partnership. This work also was supported by the UK Engineering and Physical Sciences Research Council (EPSRC) [grant number EP/P004709/1]. Emilio J. Sarabia gratefully acknowledges financial support from Universitat Politècnica de València Fellowship. Data supporting this publication can be obtained on request from cep-lab@imperial.ac.uk.

References

[1] National Statistics UK, "2017 UK greenhouse gas emissions: final figures - data tables.," 2017. [Online]. Available: https://assets.publishing.service.gov.uk/government/uploads/system/uploads/atta

chment_data/file/780395/Final_greenhouse_gas_emissions_2017_tables.xlsx. [Accessed: 03-Mar-2019].

[2] Buildings Performance Institute Europe, *EUROPE ' S BUILDINGS UNDER THE MICROSCOPE*. 2011.

[3] R. Ciconkov, "Refrigerants: There is still no vision for sustainable solutions," *Int. J. Refrig.*, vol. 86, pp. 441–448, 2018.

[4] M. Schulz and D. Kourkoulas, "Regulation (EU) No 517/2014 of the European Parliament and of the Council of 16 April 2014 on fluorinated greenhouse gases and repealing Regulation (EC) No 842/2006," *Off. J. Eur. Union*, vol. 2014, no. 517, p. L150/195-230, 2014.

[5] P. Gullo, A. Hafner, and K. Banasiak, "Transcritical R744 refrigeration systems for supermarket applications: Current status and future perspectives," vol. 93, pp. 269–310, 2018.

[6] A. Polzot, P. D'Agaro, P. Gullo, and G. Cortella, "Modelling commercial refrigeration systems coupled with water storage to improve energy efficiency and perform heat recovery," *Int. J. Refrig.*, vol. 69, pp. 313–323, 2016.

[7] J. Arias and P. Lundqvist, "Heat recovery and floating condensing in supermarkets," *Energy Build.*, vol. 38, no. 2, pp. 73–81, 2006.

[8] L. Cecchinato, M. Corradi, and S. Minetto, "Energy performance of supermarket refrigeration and air conditioning integrated systems," *Appl. Therm. Eng.*, vol. 30, no. 14–15, pp. 1946–1958, 2010.

[9] S. Sawalha, "Investigation of heat recovery in CO2trans-critical solution for supermarket refrigeration," *Int. J. Refrig.*, vol. 36, no. 1, pp. 145–156, 2013.

[10] I. Colombo, G. G. Maidment, I. Chaer, and J. M. Missenden, "Carbon dioxide refrigeration with heat recovery for supermarkets," *Int. J. Low-Carbon Technol.*, vol. 9, no. 1, pp. 38–44, 2014.

[11] A. Polzot, P. D'Agaro, and G. Cortella, "Energy Analysis of a Transcritical CO2 Supermarket Refrigeration System with Heat Recovery," *Energy Procedia*, vol. 111, no. September 2016, pp. 648–657, 2017.

[12] Y. T. Ge and S. A. Tassou, "Control optimizations for heat recovery from CO2 refrigeration systems in supermarket," *Energy Convers. Manag.*, vol. 78, pp. 245–252, 2014.

[13] S. Acha, Y. Du, and N. Shah, "Enhancing energy efficiency in supermarket refrigeration systems through a robust energy performance indicator," vol. 64, pp. 40–50, 2016.

[14] N. Purohit, P. Gullo, and M. S. Dasgupta, "Comparative Assessment of Low-GWP Based Refrigerating Plants Operating in Hot Climates," *Energy Procedia*, vol. 109, no. November 2016, pp. 138–145, 2017.

[15] P. Gullo, K. Tsamos, A. Hafnera, Y. Geb, and S. A. Tassou, "State-of-the-art technologies for transcritical refrigeration systems – a theoretical assessment of energy advantages for Assessing the feasibility of using the heat demand-outdoor European food retail industry temperature function for a long-term distric," *Energy Procedia*, vol. 123, pp. 46–53, 2017.

[16] P. Gullo, B. Elmegaard, and G. Cortella, "Energy and environmental performance assessment of R744 booster supermarket refrigeration systems operating in warm

climates," *Int. J. Refrig.*, vol. 64, pp. 61–79, 2016.

[17] M. Efstratiadi, S. Acha, N. Shah, and C. N. Markides, "Analysis of a closed-loop water-cooled refrigeration system in the food retail industry: A UK case study," *Energy*, vol. 174, pp. 1133–1144, 2019.

[18] M. Karampour and S. Sawalha, "State-of-the-art integrated CO2refrigeration system for supermarkets: A comparative analysis," *Int. J. Refrig.*, vol. 86, pp. 239–257, 2018.

[19] Shecco, "F-Gas Regulation shaking up the HVAC&R industry," p. 56, 2016.

[20] J. Arias, *Energy Usage in Supermarkets: Modelling and Field Measurements*. 2005.

[21] Z. Mylona, M. Kolokotroni, and S. A. Tassou, "Frozen food retail: Measuring and modelling energy use and space environmental systems in an operational supermarket," *Energy Build.*, vol. 144, pp. 129–143, 2017.

[22] D. B. Crawley, C. O. Pedersen, L. K. Lawrie, and F. C. Winkelmann, "EnergyPlus: Energy Simulation Program," *ASHRAE J.*, vol. 42, pp. 49–56, 2000.

[23] Y. T. Ge and S. A. Tassou, "Performance evaluation and optimal design of supermarket refrigeration systems with supermarket model 'superSim', Part I: Model description and validation," *Int. J. Refrig.*, vol. 34, no. 2, pp. 527–539, 2011.

[24] Y. T. Ge and S. A. Tassou, "Performance evaluation and optimal design of supermarket refrigeration systems with supermarket model 'SuperSim'. Part II: Model applications," *Int. J. Refrig.*, vol. 34, no. 2, pp. 540–549, 2011.

[25] Elster, "Enacto Insight." [Online]. Available: https://enactonpower.energyict.com. [Accessed: 19-Jun-2019].

[26] Accruent, "Verisae Enterprise Asset Management and Maintenance System version 50_61." [Online]. Available: https://eam.verisae.co.uk. [Accessed: 19-Jun-2019].

[27] Y. T. Ge and S. A. Tassou, "Thermodynamic analysis of transcritical CO2 booster refrigeration systems in supermarket," *Energy Convers. Manag.*, vol. 52, no. 4, pp. 1868–1875, 2011.

[28] M. Karampour and S. Sawalha, "Energy efficiency evaluation of integrated CO 2 trans-critical system in supermarkets : A field measurements and modelling analysis Évaluation de l ' efficacité énergétique d ' un système de CO2 transcritique intégré pour les supermarchés : Mesures sur si," *Int. J. Refrig.*, vol. 82, pp. 470–486, 2017.

[29] U. Kingdom and E. Consumption, "Estimates of heat use in the United Kingdom in 2013 Available at: <https://assets.publishing.service.gov.uk/government/uploads/system/uploads/attachment_data/file/386858/Estimates_of_heat_use.pdf> [accessed 28.08.2019]," no. December, pp. 93–101, 2014.

[30] Scilab Enterprises, "Scilab: Free and Open Source software for numerical computation." Orsay, France, 2012.

[31] I. H. Bell, J. Wronski, S. Quoilin, and V. Lemort, "Pure and Pseudo-pure Fluid Thermophysical Property Evaluation and the Open-Source Thermophysical Property Library CoolProp," *Ind. Eng. Chem. Res.*, vol. 53, no. 6, pp. 2498–2508, 2014.

[32] Bitzer, “BITZER software 6.5.0.” [Online]. Available: www.bitzer.de/websoftware. [Accessed: 28-Aug-2019].

[33] S. Acha, Y. Du, and N. Shah, “Enhancing energy efficiency in supermarket refrigeration systems through a robust energy performance indicator,” *Int. J. Refrig.*, vol. 64, pp. 40–50, 2016.

[34] “Met Office Integrated Data Archive System (MIDAS) Land and Marine Surface Stations Data.” [Online]. Available: http://catalogue.ceda.ac.uk/uuid/220a65615218d5c9cc9e4785a3234bd0. [Accessed: 01-Jun-2018].

[35] S. Acha and G. Bustos-turu, “Modelling Real-Time Pricing of Electricity for Energy Conservation Measures in the UK Commercial Sector,” *2016 IEEE Int. Energy Conf.*, pp. 1–6.

[36] S. Acha, A. Mariaud, N. Shah, and C. N. Markides, “Optimal design and operation of distributed low-carbon energy technologies in commercial buildings,” *Energy*, vol. 142, pp. 578–591, 2018.

[37] “DEFRA. Collection – Government Emissions conversion factors for Greenhouse gas company reporting; 2018.” [Online]. Available: https://www.gov.uk/government/publications/greenhouse-gas-reporting-conversion-factors-2018. [Accessed: 03-Mar-2019].